

Curvature tension: evidence for a closed universe

Will Handley^{1,2,3,*}

¹*Astrophysics Group, Cavendish Laboratory, J.J.Thomson Avenue, Cambridge, CB3 0HE, UK*

²*Kavli Institute for Cosmology, Madingley Road, Cambridge, CB3 0HA, UK*

³*Gonville & Caius College, Trinity Street, Cambridge, CB2 1TA, UK[†]*

(Dated: August 27, 2019)

The curvature parameter tension between Planck 2018, cosmic microwave background lensing, and baryon acoustic oscillation data is measured using the suspiciousness statistic to be 2.5 to 3σ . Conclusions regarding the spatial curvature of the universe which stem from the combination of these data should therefore be viewed with suspicion. Without CMB lensing or BAO, Planck 2018 has a moderate preference for closed universes, with Bayesian betting odds of over 50 : 1 against a flat universe, and over 2000 : 1 against an open universe.

INTRODUCTION

Quantifying the consistency between different cosmological datasets has become increasingly important in recent years. Observations of the early and late time universe give undeniably inconsistent predictions for the present day value of the expansion rate [1], a phenomenon known as the ‘‘Hubble tension’’. This paper explores a second ‘‘curvature tension’’ present within early-time observations.

Despite the long history of cosmological models which include spatial curvature [2–5], in the modern era there is a strong research community bias toward a flat universe. This is partly on theoretical grounds, since the prevailing (and very successful) inflationary theory of the primordial universe predicts a late-time cosmos which is extremely close to flat [6–8]. Curved models are also likely under-represented in the literature due in large part to the increased theoretical and numerical computational cost associated with curved cosmologies¹.

However, most of the bias toward flat cosmologies is undoubtedly derived from observational considerations, which ever since COBE [9] and BOOMERANG [10] have confirmed that the universe is consistent with a flat cosmology to within $\Omega_K = \pm 10\%$. The primary conclusion of this paper is that such a position can no longer be consistently held, as Planck 2018 cosmic microwave background data [11, 12] alone suggests a model that is closed at $\Omega_K \sim -4.5\% \pm 1.5\%$, with betting odds of 50 : 1 against a flat universe. Other datasets such as Planck 2018 CMB lensing [13] or baryon acoustic oscillations [14–16] which strongly suggest a flat universe are quantitatively inconsistent at 2.5 to 3σ with CMB data alone, and should not be confidently combined until this tension is released. Results are visualised in Fig. 1 and summarised in Figs. 2 and 3.

BACKGROUND

Cosmology with curvature ($K\Lambda$ CDM)

Under the extended Copernican principle, the universe is assumed at zeroth order to be homogeneous and isotropic at the largest scales. Einstein’s theory of general relativity under these assumptions yields the Friedmann–Lemaître–Robertson–Walker cosmology [2–5]. The metric in reduced spherical polar coordinates takes the form

$$ds^2 = dt^2 - a(t)^2 \left[\frac{dr^2}{1 - Kr^2} + r^2(d\theta^2 + \sin^2\theta d\phi^2) \right], \quad (1)$$

whereby homogeneous and isotropic spatial slices expand or contract over cosmic time t via the scale factor a . The spatial slices come in one of three forms, flat Euclidean space ($K = 0$), open hyperbolic space ($K = -1$) or closed hyperspherical space ($K = +1$). Curvature is typically quantified via its fractional contribution to the cosmic energy budget today Ω_K , which is measured as a percentage and has the opposite sign to K . In this work, I follow the notation of [18] and denote the concordance cosmology with $K = 0$ as Λ CDM, and its extension with Ω_K considered as an unknown parameter as $K\Lambda$ CDM.

Bayesian statistics

Given a set of data D and a predictive model M with parameters θ , Bayes’ theorem relates the statistical inputs to inference (the likelihood and prior) to the statistical outputs (the posterior and evidence):

$$\begin{aligned} P(D|\theta, M) \times P(\theta|M) &= P(\theta|D, M) \times P(D|M), \\ \text{Likelihood} \times \text{Prior} &= \text{Posterior} \times \text{Evidence}, \quad (2) \\ \mathcal{L} \times \pi &= \mathcal{P} \times \mathcal{Z}. \end{aligned}$$

The posterior is the central quantity in parameter estimation (what the data tell us about parameters of a model), whilst the evidence is pivotal in model comparison (what the data tell us about the relative quality of

¹ The results presented in this paper required over twelve years of high-performance computing time (or two weeks on 320 cores)

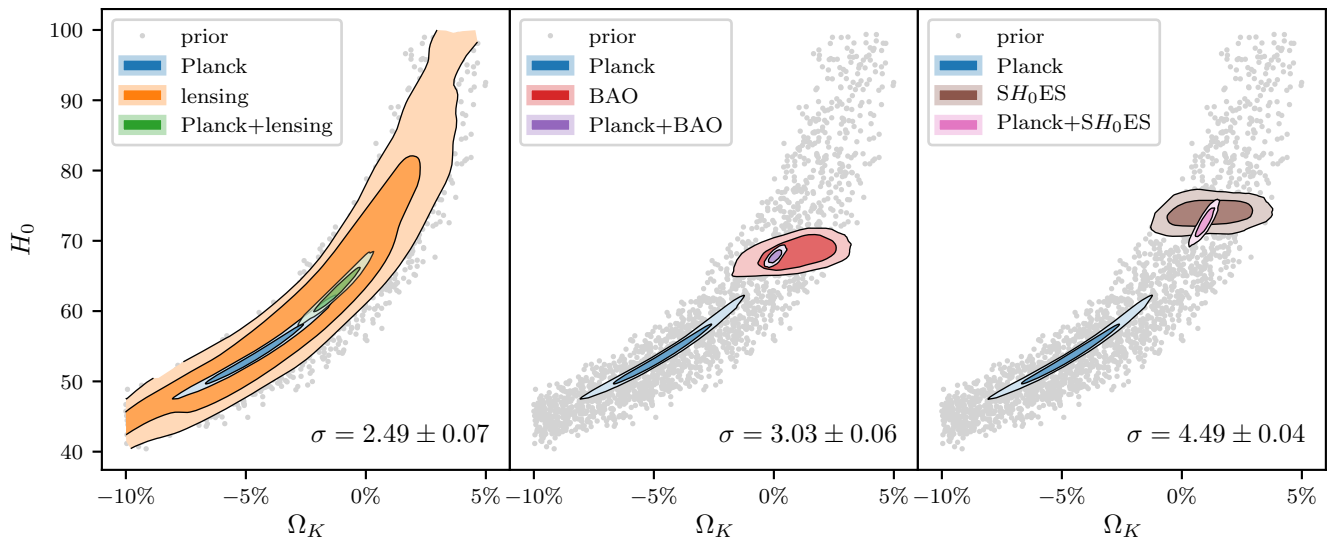


FIG. 1. Three tensions from Fig. 2 plotted in the (Ω_K, H_0) plane using `anesthetic` [17]. In the first panel, whilst the lensing posterior alone is barely distinguishable from the prior, when combined with Planck, lensing has drawn the combined posterior significantly toward flatness, at a tension of 2.5σ . The second panel shows BAO’s preference for a flat universe. The BAO posterior is disconnected from the Planck posterior, at a tension of 3σ . Finally, in the third panel the Planck- SH_0ES inconsistency in the curved case is shown to be 4.5σ .

a model) [19, 20]. The evidence ratio gives the Bayesian betting odds one would assign between two competing models, assuming equal *a priori* model probability.

Parameter estimation is typically performed by compressing the high-dimensional posterior into a set of representative samples via a Markov-Chain Monte-Carlo process [21]. The evidence is derived from the likelihood by marginalising over the prior

$$\mathcal{Z} = \int \mathcal{L}(\theta)\pi(\theta) d\theta = \langle \mathcal{L} \rangle_{\pi}, \quad (3)$$

which may be computed numerically via a Laplace approximation [22], Savage Dickey ratio [23], nearest-neighbour volume estimation [24, 25] or nested sampling [19, 26–31]. If one has access to the evidence, then it is straightforward to compute the Kullback-Leibler divergence

$$\mathcal{D} = \int \mathcal{P}(\theta) \log \frac{\mathcal{P}(\theta)}{\pi(\theta)} d\theta = \left\langle \log \frac{\mathcal{P}}{\pi} \right\rangle_{\mathcal{P}}, \quad (4)$$

which quantifies the degree of compression from prior to posterior provided by the data.

As a model comparison tool, the evidence naturally quantifies Occam’s razor, incorporating a parameter volume-based penalty that penalises models with unnecessary constrained parameters. This penalty factor may be approximated using the difference in KL divergence between models. For further detail on Bayesian statistics, readers are recommended references [22, 32–34].

Tension quantification

The Bayesian evidence from Eq. (3) also appears in tension quantification [35, 37–42]. The Bayes ratio

$$R = \frac{P(D_2|D_1)}{P(D_2)} = \frac{P(D_1|D_2)}{P(D_1)} = \frac{\mathcal{Z}_{12}}{\mathcal{Z}_1\mathcal{Z}_2}, \quad (5)$$

quantifies the compatibility of two datasets D_1 and D_2 by giving a Bayesian’s relative confidence in their combination. As with many Bayesian quantities, R is naturally prior dependent [35]. In the absence of well-motivated priors, or if deliberately over-wide ranges on parameters are used (as is often the case in cosmology), the prior dependency can be removed from R using the KL divergence from Eq. (4). Dividing R by the information ratio I gives the suspiciousness S

$$S = \frac{R}{I}, \quad \log I = \mathcal{D}_1 + \mathcal{D}_2 - \mathcal{D}_{12}, \quad (6)$$

Using a Gaussian analogy, one may calibrate S into a tension probability p and convert this into an equivalent “sigma value” via the survival function of the chi-squared distribution

$$p = \int_{d-2\log S}^{\infty} \chi_d^2(x) dx, \quad \sigma = \sqrt{2}\text{Erfc}^{-1}(p), \quad (7)$$

where Erfc^{-1} is the inverse complementary error function and d is quantified by the Bayesian model dimensionality [36, 43–46]

$$d = \tilde{d}_1 + \tilde{d}_2 - \tilde{d}_{12}, \quad \tilde{d}/2 = \langle (\log \mathcal{L})^2 \rangle_{\mathcal{P}} - \langle \log \mathcal{L} \rangle_{\mathcal{P}}^2. \quad (8)$$

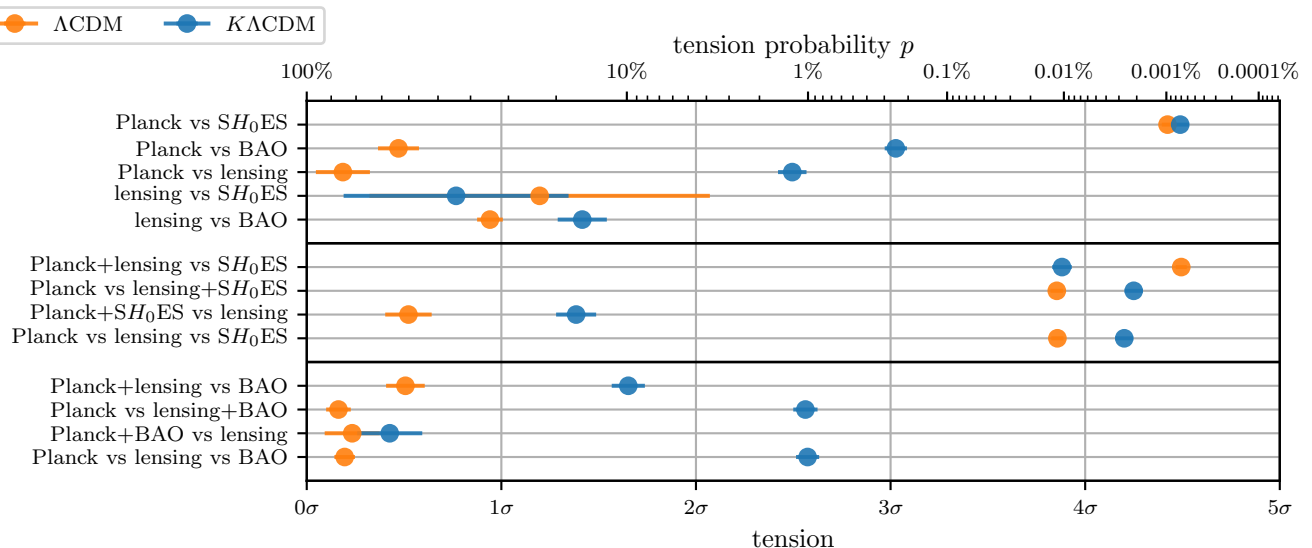


FIG. 2. Parameter tensions computed using `anesthetic` [17]. The top line shows the severe tension between SH_0ES and Planck detailed in [35, 36] updated for Planck 2018 data. For $\Lambda CD M$ Planck, lensing and BAO are all consistent. For $K\Lambda CD M$, Planck and BAO are strongly inconsistent, whilst Planck and lensing are moderately inconsistent. The ninth and final rows indicate the triple tension from Eq. (9), and show strong mutual inconsistency between Planck, lensing and SH_0ES , and moderate mutual inconsistency between Planck, lensing and BAO. Curvature in general enhances tension, but relaxes it for Planck+lensing vs SH_0ES . The large error bars for lensing vs SH_0ES occur due to the fact their shared constrained parameters have $\tilde{d} \ll 1$.

Abbrev.	Description
Planck [12]	Temperature and polarization anisotropies in the CMB measured from the publicly available baseline Planck 2018 TTTEEE+lowE likelihood.
lensing [13]	Planck 2018 baseline CMB lensing likelihood.
BAO [14–16]	Baryon Acoustic Oscillation and Redshift Space Distortion measurements from the Baryon Oscillation Spectroscopic Survey (BOSS) DR12.
SH_0ES [59]	Supernovae and H_0 for the Equation of State: local cosmic distance ladder measurements of the expansion rate, using type Ia SNe calibrated by variable Cepheid stars. Implemented as a Gaussian likelihood.

TABLE I. Abbreviations, citations and descriptions for observational datasets used in this analysis.

The differences in model dimensionalities recover the number of shared constrained parameters. See [35, 36] for a more detailed discussion of tension and model dimensionality. Other tension metrics are also available [47–58].

In this work the “triple tension” is also introduced to quantify the tension between three datasets simultaneously, extending the definition of R , I and d from Eqs. (5), (6) and (8) when necessary to

$$R = \frac{\mathcal{Z}_{123}}{\mathcal{Z}_1 \mathcal{Z}_2 \mathcal{Z}_3}, \quad \log I = \mathcal{D}_1 + \mathcal{D}_2 + \mathcal{D}_3 - \mathcal{D}_{123}, \quad (9)$$

$$d = \tilde{d}_1 + \tilde{d}_2 + \tilde{d}_3 - \tilde{d}_{123},$$

with obvious generalisation to four or more parameters.

METHODOLOGY

The observational datasets used for this analysis are described in Tab. I. Note that throughout this paper “lensing” is an abbreviation for “Planck CMB lensing”.

Bayesian evidences and posteriors are computed using nested sampling [19] provided by `CosmoChord`[60], an extension of `CosmoMC` [21] using `PolyChord` [27, 28] to sample efficiently in high dimensions and exploit the fast-slow cosmological parameter hierarchy [61]. The post-processing computations for the evidence, KL divergence and Bayesian model dimensionality detailed in Figs. 2 and 3, as well as the posterior plots in Figs. 1 and 4 are computed using the `anesthetic` [17] software package.

All cosmological and nuisance parameters are varied in the nested sampling runs. The cosmological prior widths (visualised in Fig. 4) are narrower than the `CosmoMC` defaults. This is necessary since nested sampling begins by exploring the deep tails of the distribution. In these regions unphysical and unforeseen combinations of parameters causes cosmology codes to fail. Whilst flat cosmology codes have been extensively stress-tested by nested sampling, the curved branches have not. Since the priors are wide enough to fully encompass the posteriors, there would be little quantitative effect on the conclusions of this paper from using a wider set of priors.

All inference products required to compute results are available for download from Zenodo [62].

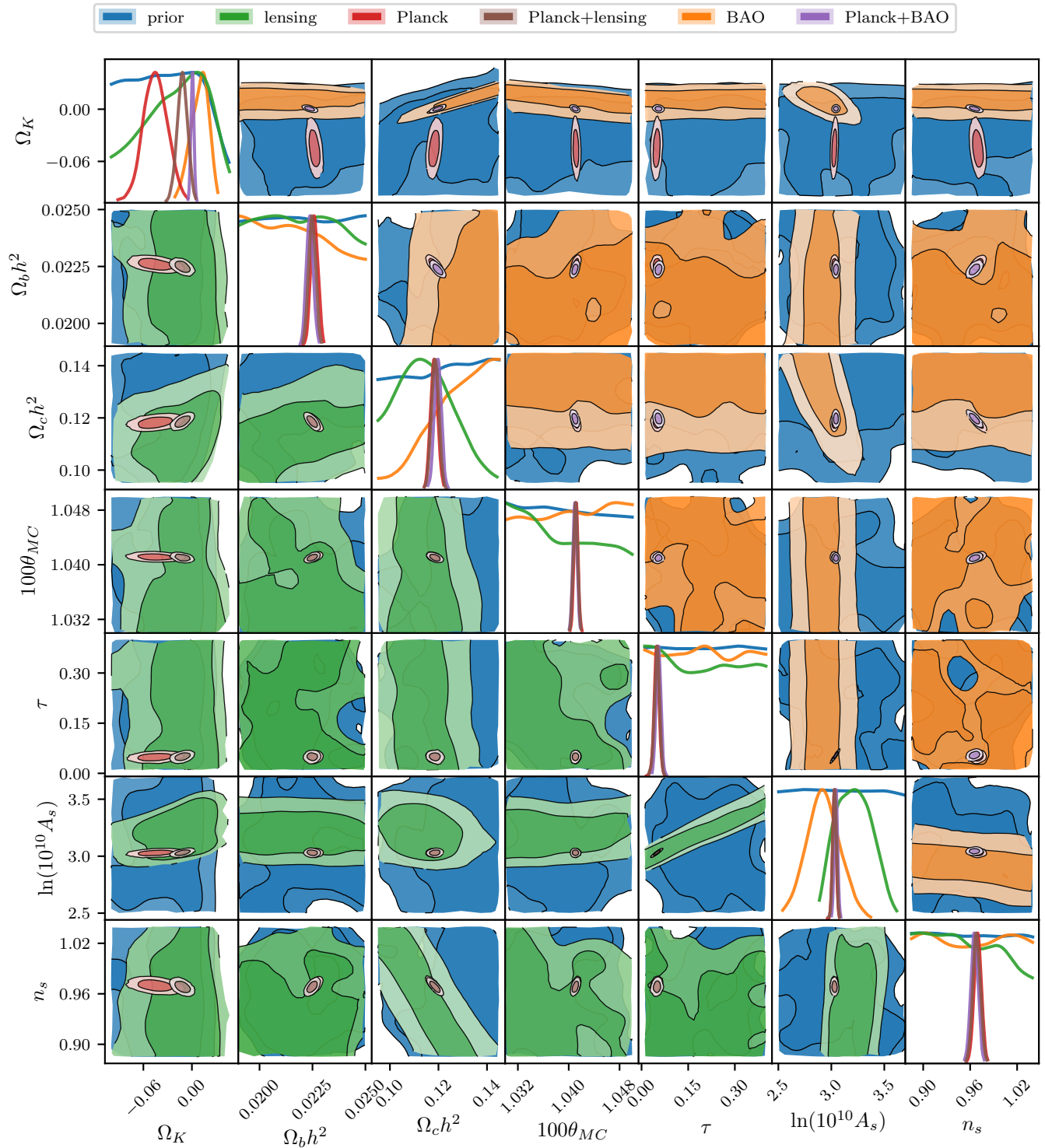


FIG. 4. One- and two-dimensional marginalised priors and posteriors for the seven cosmological parameters of the Λ CDM cosmology, plotted with `anesthetic` [17]. Plots on the diagonal are one-dimensional marginalisations, and off-diagonal plots are contour plots showing marginal iso-probability contours containing 68% and 95% of the marginalised posterior mass. The prior in blue and the Planck posterior in red are included in all plots, below-diagonal elements show lensing posteriors, above-diagonal elements show posteriors for BAO. The left-most column and top-most row detail curvature, where the tension between the posteriors can be seen clearly. The remaining parameters show no discernible tensions. Lensing constrains approximately two parameters, a linear combination of $\Omega_c h^2$ and n_s , and a linear combination of $\ln(10^{10} A_s)$ and τ , which is reflected in the Bayesian model dimensionality of $\tilde{d}_{\text{lensing}} = 1.8 \pm 1$. BAO has a model dimensionality of $\tilde{d}_{\text{BAO}} = 2.6 \pm 0.1$, consistent with its constraints on $\ln(10^{10} A_s)$ and Ω_K , and its partial constraint on $\Omega_c h^2$.

- * wh260@mrao.cam.ac.uk
† <https://www.kicc.cam.ac.uk/directory/wh260>
- [1] L. Verde, T. Treu, and A. G. Riess. Tensions between the Early and the Late Universe. *arXiv e-prints*, art. arXiv:1907.10625, Jul 2019.
 - [2] A. Friedmann. Über die Möglichkeit einer Welt mit konstanter negativer Krümmung des Raumes. *Zeitschrift für Physik*, 21:326–332, December 1924. doi:10.1007/BF01328280.
 - [3] G. Lemaitre. Un Univers homogène de masse constante et de rayon croissant rendant compte de la vitesse radiale des nébuleuses extra-galactiques. *Annales de la Société Scientifique de Bruxelles*, 47:49–59, 1927.
 - [4] H. P. Robertson. On the Foundations of Relativistic Cosmology. *Proceedings of the National Academy of Science*, 15(11):822–829, Nov 1929. doi:10.1073/pnas.15.11.822.
 - [5] A. G. Walker. On Milne’s Theory of World-Structure. *Proceedings of the London Mathematical Society, (Series 2) volume 42, p. 90–127*, 42:90–127, 1937. doi:10.1112/plms/s2-42.1.90.
 - [6] A. A. Starobinskiĭ. Spectrum of relict gravitational radiation and the early state of the universe. *Soviet Journal of Experimental and Theoretical Physics Letters*, 30:682, December 1979.
 - [7] A. H. Guth. Inflationary universe: A possible solution to the horizon and flatness problems. *Phys. Rev. D*, 23:347–356, January 1981. doi:10.1103/PhysRevD.23.347.
 - [8] A. D. Linde. A new inflationary universe scenario: A possible solution of the horizon, flatness, homogeneity, isotropy and primordial monopole problems. *Phys. Lett. B*, 108:389–393, February 1982. doi:10.1016/0370-2693(82)91219-9.
 - [9] C. L. Bennett, A. J. Banday, K. M. Gorski, G. Hinshaw, P. Jackson, P. Keegstra, A. Kogut, G. F. Smoot, D. T. Wilkinson, and E. L. Wright. Four-Year COBE DMR Cosmic Microwave Background Observations: Maps and Basic Results. *ApJ*, 464:L1, June 1996. doi:10.1086/310075.
 - [10] BOOMERANG Collaboration. A Measurement by BOOMERANG of Multiple Peaks in the Angular Power Spectrum of the Cosmic Microwave Background. *ApJ*, 571:604–614, June 2002. doi:10.1086/340118.
 - [11] Planck Collaboration. Planck 2018 results. VI. Cosmological parameters. *arXiv e-prints*, art. arXiv:1807.06209, Jul 2018.
 - [12] Planck Collaboration. Planck 2018 results. V. CMB power spectra and likelihoods. *arXiv e-prints*, art. arXiv:1907.12875, Jul 2019.
 - [13] Planck Collaboration. Planck 2018 results. VIII. Gravitational lensing. *arXiv e-prints*, art. arXiv:1807.06210, Jul 2018.
 - [14] Shadab Alam and et al. The clustering of galaxies in the completed SDSS-III Baryon Oscillation Spectroscopic Survey: cosmological analysis of the DR12 galaxy sample. *MNRAS*, 470:2617–2652, September 2017. doi:10.1093/mnras/stx721.
 - [15] Florian Beutler, Chris Blake, Matthew Colless, D. Heath Jones, Lister Staveley-Smith, Lachlan Campbell, Quentin Parker, Will Saunders, and Fred Watson. The 6dF Galaxy Survey: baryon acoustic oscillations and the local Hubble constant. *MNRAS*, 416:3017–3032, October 2011. doi:10.1111/j.1365-2966.2011.19250.x.
 - [16] Ashley J. Ross, Lado Samushia, Cullan Howlett, Will J. Percival, Angela Burden, and Marc Manera. The clustering of the SDSS DR7 main Galaxy sample - I. A 4 per cent distance measure at $z = 0.15$. *MNRAS*, 449:835–847, May 2015. doi:10.1093/mnras/stv154.
 - [17] Will Handley. anesthetic: nested sampling visualisation. *The Journal of Open Source Software*, 4(37), Jun 2019. doi:10.21105/joss.01414. URL <http://dx.doi.org/10.21105/joss.01414>.
 - [18] Will Handley. Primordial power spectra for curved inflating universes. *arXiv e-prints*, art. arXiv:1907.08524, Jul 2019.
 - [19] John Skilling. Nested sampling for general bayesian computation. *Bayesian Anal.*, 1(4):833–859, 12 2006. doi:10.1214/06-BA127. URL <https://doi.org/10.1214/06-BA127>.
 - [20] R. Trotta. Bayes in the sky: Bayesian inference and model selection in cosmology. *Contemporary Physics*, 49:71–104, March 2008. doi:10.1080/00107510802066753.
 - [21] Antony Lewis and Sarah Bridle. Cosmological parameters from CMB and other data: A Monte Carlo approach. *Phys. Rev.*, D66:103511, 2002. doi:10.1103/PhysRevD.66.103511.
 - [22] D.J.C. MacKay, D.J.C.M. Kay, and Cambridge University Press. *Information Theory, Inference and Learning Algorithms*. Cambridge University Press, 2003. ISBN 9780521642989. URL <https://books.google.co.uk/books?id=AKuMj4PN EMC>.
 - [23] Roberto Trotta. Applications of Bayesian model selection to cosmological parameters. *MNRAS*, 378:72–82, June 2007. doi:10.1111/j.1365-2966.2007.11738.x.
 - [24] Alan Heavens, Yabebal Fantaye, Arrikrishna Mootoovaloo, Hans Eggers, Zafiiarah Hosenie, Steve Kroon, and Elena Sellentin. Marginal Likelihoods from Monte Carlo Markov Chains. *arXiv e-prints*, art. arXiv:1704.03472, April 2017.
 - [25] Alan Heavens, Yabebal Fantaye, Elena Sellentin, Hans Eggers, Zafiiarah Hosenie, Steve Kroon, and Arrikrishna Mootoovaloo. No Evidence for Extensions to the Standard Cosmological Model. *Phys. Rev. Lett.*, 119:101301, September 2017. doi:10.1103/PhysRevLett.119.101301.
 - [26] F. Feroz, M. P. Hobson, and M. Bridges. MULTINEST: an efficient and robust Bayesian inference tool for cosmology and particle physics. *MNRAS*, 398:1601–1614, October 2009. doi:10.1111/j.1365-2966.2009.14548.x.
 - [27] W. J. Handley, M. P. Hobson, and A. N. Lasenby. POLYCHORD: nested sampling for cosmology. *MNRAS*, 450:L61–L65, June 2015. doi:10.1093/mnras/15v047.
 - [28] W. J. Handley, M. P. Hobson, and A. N. Lasenby. POLYCHORD: next-generation nested sampling. *MNRAS*, 453:4384–4398, November 2015. doi:10.1093/mnras/stv1911.
 - [29] Brendon J Brewer, Livia B Pártay, and Gábor Csányi. Diffusive nested sampling. *Statistics and Computing*, 21(4):649–656, 2011.
 - [30] Brendon J. Brewer and Daniel Foreman-Mackey. DNest4: Diffusive Nested Sampling in C++ and Python. *arXiv e-prints*, art. arXiv:1606.03757, June 2016.
 - [31] Joshua S Speagle. dynesty: A Dynamic Nested Sampling Package for Estimating Bayesian Posteriors and Evidences. *arXiv e-prints*, art. arXiv:1904.02180, Apr 2019.
 - [32] M.P. Hobson, A.H. Jaffe, A.R. Liddle, P. Mukherjee,

- and D. Parkinson. *Bayesian Methods in Cosmology*. Bayesian Methods in Cosmology. Cambridge University Press, 2010. ISBN 9780521887946. URL <https://books.google.co.uk/books?id=RzehSUtgxvsC>.
- [33] Roberto Trotta. Bayesian Methods in Cosmology. *arXiv e-prints*, art. arXiv:1701.01467, Jan 2017.
- [34] D. Sivia and J. Skilling. *Data Analysis: A Bayesian Tutorial*. Oxford science publications. OUP Oxford, 2006. ISBN 9780198568315. URL <https://books.google.co.uk/books?id=LYMSDAAAQBAJ>.
- [35] Will Handley and Pablo Lemos. Quantifying tensions in cosmological parameters: Interpreting the DES evidence ratio. *Phys. Rev. D*, 100:043504, Aug 2019.
- [36] Will Handley and Pablo Lemos. Quantifying dimensionality: Bayesian cosmological model complexities. *Phys. Rev. D*, 100(2):023512, Jul 2019. doi:10.1103/PhysRevD.100.023512.
- [37] Phil Marshall, Nutan Rajguru, and Anže Slosar. Bayesian evidence as a tool for comparing datasets. *Phys. Rev. D*, 73:067302, March 2006. doi:10.1103/PhysRevD.73.067302.
- [38] Licia Verde, Pavlos Protopapas, and Raul Jimenez. Planck and the local Universe: Quantifying the tension. *Physics of the Dark Universe*, 2:166–175, September 2013. doi:10.1016/j.dark.2013.09.002.
- [39] Licia Verde. Precision cosmology, accuracy cosmology and statistical cosmology. *Proceedings of the International Astronomical Union*, 10(S306):223234, 2014. doi:10.1017/S1743921314013593.
- [40] M. Raveri. Are cosmological data sets consistent with each other within the Λ cold dark matter model? *Phys. Rev. D*, 93(4):043522, February 2016. doi:10.1103/PhysRevD.93.043522.
- [41] S. Seehars, S. Grandis, A. Amara, and A. Refregier. Quantifying concordance in cosmology. *Phys. Rev. D*, 93(10):103507, May 2016. doi:10.1103/PhysRevD.93.103507.
- [42] T. M. C. Abbott, F. B. Abdalla, A. Alarcon, J. Aleksić, S. Allam, S. Allen, A. Amara, J. Annis, J. Asorey, S. Avila, and et al. Dark Energy Survey year 1 results: Cosmological constraints from galaxy clustering and weak lensing. *Phys. Rev. D*, 98(4):043526, Aug 2018. doi:10.1103/PhysRevD.98.043526.
- [43] Andrew Gelman, John B. Carlin, Hal S. Stern, and Donald B. Rubin. *Bayesian Data Analysis*. Chapman and Hall/CRC, 2nd ed. edition, 2004.
- [44] David J. Spiegelhalter, Nicola G. Best, Bradley P. Carlin, and Angelika van der Linde. The deviance information criterion: 12 years on. *Journal of the Royal Statistical Society: Series B (Statistical Methodology)*, 76(3):485–493. doi:10.1111/rssb.12062. URL <https://rss.onlinelibrary.wiley.com/doi/abs/10.1111/rssb.12062>.
- [45] Martin Kunz, Roberto Trotta, and David R. Parkinson. Measuring the effective complexity of cosmological models. *Phys. Rev. D*, 74:023503, Jul 2006. doi:10.1103/PhysRevD.74.023503.
- [46] Andrew R. Liddle. Information criteria for astrophysical model selection. *MNRAS*, 377:L74–L78, May 2007. doi:10.1111/j.1745-3933.2007.00306.x.
- [47] T. Charnock, R. A. Battye, and A. Moss. Planck data versus large scale structure: Methods to quantify discordance. *Phys. Rev. D*, 95(12):123535, June 2017. doi:10.1103/PhysRevD.95.123535.
- [48] Henry F. Inman and Edwin L. Bradley Jr. The overlapping coefficient as a measure of agreement between probability distributions and point estimation of the overlap of two normal densities. *Communications in Statistics - Theory and Methods*, 18(10):3851–3874, 1989. doi:10.1080/03610928908830127. URL <https://doi.org/10.1080/03610928908830127>.
- [49] Richard A. Battye, Tom Charnock, and Adam Moss. Tension between the power spectrum of density perturbations measured on large and small scales. *Phys. Rev. D*, 91:103508, May 2015. doi:10.1103/PhysRevD.91.103508.
- [50] Sebastian Seehars, Adam Amara, Alexandre Refregier, Aseem Paranjape, and Joël Akeret. Information gains from cosmic microwave background experiments. *Phys. Rev. D*, 90:023533, July 2014. doi:10.1103/PhysRevD.90.023533.
- [51] Andrina Nicola, Adam Amara, and Alexandre Refregier. Consistency tests in cosmology using relative entropy. *J. Cosmology Astropart. Phys.*, 2019(1):011, Jan 2019. doi:10.1088/1475-7516/2019/01/011.
- [52] Martin Kunz, Roberto Trotta, and David R. Parkinson. Measuring the effective complexity of cosmological models. *Phys. Rev. D*, 74:023503, July 2006. doi:10.1103/PhysRevD.74.023503.
- [53] N. V. Karpenka, F. Feroz, and M. P. Hobson. Testing the mutual consistency of different supernovae surveys. *MNRAS*, 449:2405–2412, May 2015. doi:10.1093/mnras/stv415.
- [54] Niall MacCrann, Joe Zuntz, Sarah Bridle, Bhuvnesh Jain, and Matthew R. Becker. Cosmic discordance: are Planck CMB and CFHTLenS weak lensing measurements out of tune? *MNRAS*, 451:2877–2888, August 2015. doi:10.1093/mnras/stv1154.
- [55] Saroj Adhikari and Dragan Huterer. A new measure of tension between experiments. *J. Cosmology Astropart. Phys.*, 2019(1):036, Jan 2019. doi:10.1088/1475-7516/2019/01/036.
- [56] Marian Douspis, Laura Salvati, and Nabila Aghanim. On the Tension between Large Scale Structures and Cosmic Microwave Background. *PoS, EDSU2018:037*, 2018. doi:10.22323/1.335.0037.
- [57] Marco Raveri and Wayne Hu. Concordance and discordance in cosmology. *Phys. Rev. D*, 99(4):043506, Feb 2019. doi:10.1103/PhysRevD.99.043506.
- [58] M. P. Hobson, S. L. Bridle, and O. Lahav. Combining cosmological data sets: hyperparameters and Bayesian evidence. *MNRAS*, 335:377–388, September 2002. doi:10.1046/j.1365-8711.2002.05614.x.
- [59] SH₀ES Collaboration. New Parallaxes of Galactic Cepheids from Spatially Scanning the Hubble Space Telescope: Implications for the Hubble Constant. *ApJ*, 855:136, March 2018. doi:10.3847/1538-4357/aaadb7.
- [60] W. J. Handley. Cosmochord 1.15, January 2019. URL <https://doi.org/10.5281/zenodo.3370086>.
- [61] Antony Lewis. Efficient sampling of fast and slow cosmological parameters. *Phys. Rev.*, D87:103529, 2013. doi:10.1103/PhysRevD.87.103529.
- [62] Will Handley. Curvature tension: evidence for a closed universe (supplementary inference products), August 2019. URL <https://doi.org/10.5281/zenodo.3371152>.